

Structural Basis for the Interaction Between Carbonic Anhydrase and 1,2,3,4-tetrahydroisoquinolin-2-ylsulfonamides[†]

Pavel Mader,[‡] Jiří Brynda,^{‡,§} Rosaria Gitto,^{||} Stefano Agnello,^{||} Petr Páchl,[‡] Claudiu T. Supuran,[⊥] Alba Chimirri,^{||} and Pavlína Řezáčová^{‡*,†,§}

[‡]Department of Structural Biology, Institute of Molecular Genetics, Academy of Sciences of the Czech Republic, Prague, Czech Republic

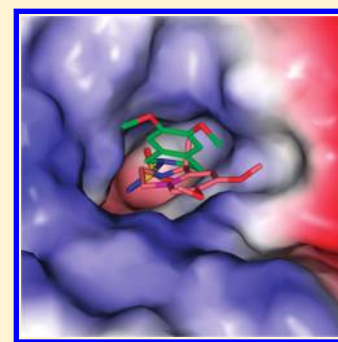
[§]Structural Biology Team, Institute of Organic Chemistry and Biochemistry, Academy of Sciences of the Czech Republic, Prague, Czech Republic

^{||}Dipartimento Farmaco-Chimico, Università di Messina, Messina, Italy

[⊥]Laboratorio di Chimica Bioinorganica, Università degli Studi di Firenze, Firenze, Italy

S Supporting Information

ABSTRACT: Isoquinolinesulfonamides inhibit human carbonic anhydrases (hCAs) and display selectivity toward therapeutically relevant isozymes. The crystal structure of hCA II in complex with 6,7-dimethoxy-1-methyl-1,2,3,4-tetrahydroisoquinolin-2-ylsulfonamide revealed unusual inhibitor binding. Structural analyses allowed for discerning the fine details of the inhibitor binding mode to the active site, thus providing clues for the future design of even more selective inhibitors for druggable isoforms such as the cancer associated hCA IX and neuronal hCA VII.



INTRODUCTION

Human carbonic anhydrases (hCAs, EC 4.2.1.1) form a family of zinc metalloenzymes that play an important role in several physiological and pathological processes. To date, 15 human isozymes have been identified displaying differences in activity, subcellular localization, and tissue expression profiles. They play key roles in intracellular and extracellular pH homeostasis, in the transport of CO₂ and bicarbonate in respiration, and in several biochemical pathways where either CO₂ or bicarbonate is required,¹ with bone resorption, the production of gastric acid, renal acidification, and lipogenesis representing just a few examples. Immense experimental evidence also suggested the role of hCAs in various pathological processes (e.g., tumorigenicity, obesity, and epilepsy). Thus, many isozymes are established diagnostic and therapeutic targets.

About 30 carbonic anhydrase inhibitors are clinically used as antiglaucoma drugs (targeting hCA II, hCA IV, and hCA XII), anticonvulsants (targeting hCA II, hCA VII, and hCA XIV), and antiobesity agents (targeting hCA VA and hCA VB).^{2,3} The classical carbonic anhydrase inhibitors (CAIs), which have been known for more than 50 years and which are used in therapy, contain a sulfonamide (e.g., acetazolamide) or a sulfamate (e.g., topiramate) moiety coordinating the Zn(II) ion located in the enzyme catalytic site (reviewed in refs 4 and 5). Nevertheless, most of currently used CA inhibitors lack selectivity, presenting numerous unwanted side effects. The design of a novel generation

of isozyme-selective CA inhibitors is the current challenge in the development of new therapeutic agents able to inhibit specific isozymes.

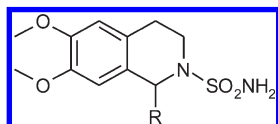
Recently, several isozymes became popular targets for inhibitor development. Isozyme CA XIV is a transmembrane isoform highly abundant in neurons and axons in the human brain,⁶ where it seems to play an important role in modulating excitatory synaptic transmission, and is an emerging target for neuroprotective agents.⁷ Neuronal hCA VII is an important target for the development of anticonvulsant agents and neuropathic pain killers.⁸ Two transmembrane hCA isozymes (hCA IX and hCA XII) are associated with cancer, and their role in tumor progression was recently established.⁹ Targeting these tumor-specific hCA isozymes with specific inhibitors thus became a promising strategy for cancer therapy.^{10–12}

In our previous work, we explored isoquinoline sulfonamides that showed inhibitory effects against some hCA isozymes at nanomolar concentrations.^{13,14} One of the most interesting results was the identification of new CAIs displaying a high potency and selectivity toward some therapeutically relevant isozymes (hCA VII, hCA IX, and hCA XIV)^{13,14} over the widespread hCA II isozyme. The crystal structure of 6,7-dimethoxy-1,2,3,4-tetrahydroisoquinolin-2-ylsulfonamide as a prototype of this series in

Received: January 10, 2011

Published: March 11, 2011

Table 1. Inhibition of hCA II, hCA VII, hCA IX, and hCA XIV Isoforms by Tetrahydroisoquinoline Derivatives (**1** and **2**), Acetazolamide, and Topiramate



compd	R	K_i (nM) ^a			
		hCA II ^b	hCA VII ^c	hCA IX ^b	hCA XIV ^b
1	H	94.5	5.4	9.5	9.8
2	methyl	87.3	6.4	9.4	9.6
acetazolamide		12	2.5	25	41
topiramate		10	0.9	58	1460

^aExperimental errors are $\pm 10\%$ of the reported value, from three different assays. Recombinant full length hCAs II, VII, and XIV and the catalytic domain of hCA IX were used. ^bValues from ref 13. ^cValues from ref 14.

complex with hCA II provided valuable structural information on the protein–inhibitor interaction. Subsequent docking studies suggested that the nature of the C-1 substituent on the isoquinoline scaffold affects the hCA isoform specificity.¹³

To understand the structural basis of interaction of isoquinoline sulfonamide derivatives with hCAs, we report the crystal structure of hCA II in complex with 6,7-dimethoxy-1-methyl-1,2,3,4-tetrahydroisoquinolin-2-ylsulfonamide. Comparison of the inhibitor position within the enzyme active site cavity with the previously determined crystal structure of the prototype compound lacking the methyl substitution on the C-1 position (PDB code 3IGP¹³) revealed striking differences in the inhibitor binding mode. These results obtained by protein crystallography could help in the elucidation of the isoform selectivity of other alkyl-substituted compounds at the C-1 position observed previously and also should be beneficial in future rational drug design.

RESULTS AND DISCUSSION

Compounds **1** and **2** were synthesized following the previously reported procedure.¹³ Both **1** and **2** show inhibitory efficacy toward various CA isoforms *in vitro*, but their selectivity differs substantially from well-known CAIs such as acetazolamide and topiramate (Table 1). Compounds **1** and **2** were able to inhibit the widely distributed hCA II with K_i of 94.5 and 87.3 nM, respectively, but interestingly they were able to inhibit druggable isoforms hCA VII, hCA IX, and hCA XIV with even higher potency (K_i in the nanomolar range).

Structural information on **1** binding to hCA II was published by us previously.¹³ In the present work, the crystal structure of hCA II in complex with 6,7-dimethoxy-1-methyl-1,2,3,4-tetrahydroisoquinolin-2-ylsulfonamide (**2**) was determined and refined using diffraction data to 1.47 Å resolution (Figure 1). Well-defined, non-protein electron densities indicated the binding of an inhibitor molecule into the primary binding site in the enzyme active site and the secondary inhibitor binding site on the surface of the protein molecule near the N-terminus. The secondary binding site, also reported for other hCA II–inhibitor crystal

structures (e.g., PDB codes 3HS4¹⁵ and 2QOA¹⁶), most likely has no biological relevance and represents a crystallization artifact caused by high concentrations of the inhibitor used in the cocrystallization experiments.

As shown in Figure 1C, **2** binds into the cavity of the hCA II active site with the deeply buried sulfonamide group. The ionized nitrogen atom of the sulfonamide moiety is coordinated to the zinc ion at ~ 2.0 Å. The sulfonamide nitrogen also accepts a hydrogen bond from the hydroxyl group of Thr199 side chain, and one oxygen atom from the sulfonamide moiety forms a hydrogen bond with backbone amine group of Thr199. Positions of the N ϵ atoms of His 94 and His 96 and N δ atom of His 119 form a ligand field, which dictates the position of a coordinated Zn²⁺ cation and consequently determines the position of acidic group of the sulfonamide to complete the tetrahedral coordination of the central zinc ion. The position of the sulfonamide group and the key hydrogen bond network in the active site are highly conserved in all known structures of hCA II–sulfonamide complexes deposited in PDB.^{17–20}

In addition to the polar interactions mediated by the sulfonamide group, the oxygen of the 6-methoxy group of **2** (labeled OAK in Figure 1B) is stabilizing the inhibitor in proximity of β -sheet 8 by forming an additional polar interaction (2.73 Å) with side chain N δ atom of Asn 67. N ϵ atom of Gln 92 is positioned 2.89 Å from the oxygen atom (labeled OAL in Figure 1B) of the other methoxy group at the 7-position; however, the overall geometry does not allow additional polar interaction to be formed between these two atoms. Several hydrophobic interactions of the substituted isoquinoline moiety with residues of the central β -sheet (mainly with Gln 92 and Val 121) stabilize the inhibitor within the active site cavity.

Compound **2** was synthesized as a racemic mixture of the two enantiomers and has been used in crystallization trials. Interestingly, the high resolution crystal structure revealed that the absolute configuration of **2** bound in the active site was *R* while the inhibitor bound on the surface was the *S* enantiomer. This suggests that only one enantiomer represents an active compound. This subject will be addressed in future research aimed at the enantiomeric resolution of the active isoquinoline sulfonamide based compounds.¹³

We compared the hCA II–**2** complex with the structure containing the parent, the unsubstituted isoquinoline based inhibitor **1** (6,7-dimethoxy-1,2,3,4-tetrahydroisoquinolin-2-yl-sulfonamide; PDB code 3IGP¹³). Although the two compounds differ only by the presence of the methyl group substitution at C-1 in **2** (see Table 1), their binding modes in the enzyme active site are quite dissimilar (Figure 2).

The position of the sulfonamide group is well conserved in the two crystal structures; the major difference is in the arrangement of the isoquinoline moiety within the active site cavity. The rearrangement of **2** compared to **1** is achieved by the rotation around the covalent bond between sulfur and nitrogen atoms (atoms SAS and NAR in Figure 1B) accompanied by the change of the isoquinoline ring puckering. The three dihedral angles defined by atoms of nonaromatic ring CAQ–NAR–CAJ–CAI, CAP–CAQ–NAR–CAJ, and NAR–CAJ–CAI–CAM (Figure 1B) are 0.2°, 30.4°, and –30.8° for **1** and –75.2°, 52.0°, 52.8° for **2**. The substantial change in position of **2** with respect to **1** within the hCA II active site can also be documented by a distance of more than 4 Å between the two corresponding methoxy oxygen atoms in **1** and **2**, respectively (atoms OAL and OAK in Figure 1B).

The isoquinoline moiety of **1** forms numerous van der Waals interactions with residues Gln 92, Val 121 located on the bottom

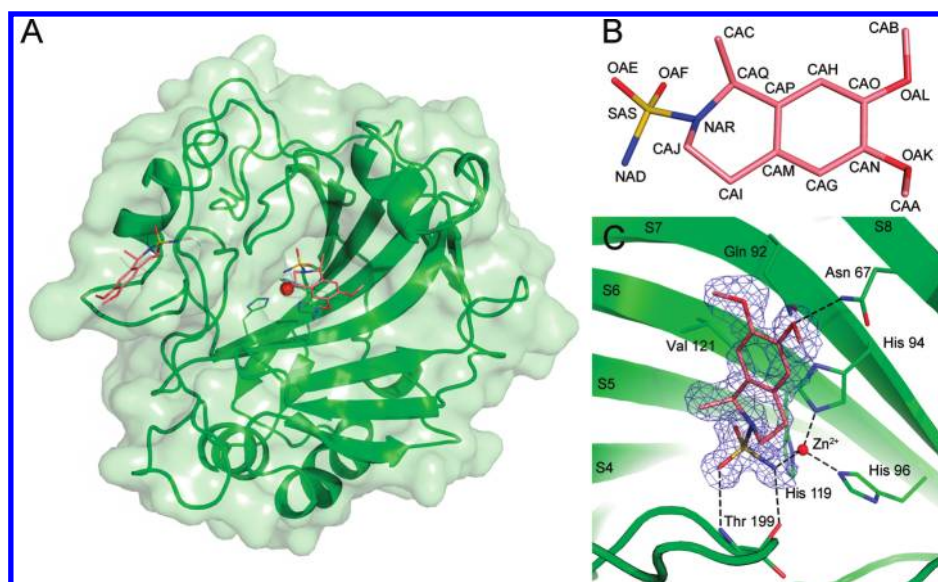


Figure 1. (A) Overall view of structure of hCA II in complex with **2**. The main chain of the protein is represented by a ribbon and a transparent solvent accessible surface. The zinc ion is shown as a red sphere with three coordinating histidine residues in sticks. Two molecules of inhibitor **2** bound to hCA II are shown in the stick model with carbon atoms colored salmon and oxygen and nitrogen atoms colored red and blue, respectively. (B) Structure of **2** with atom labels used in the crystal structure coordinate file. (C) Detail of the hCA II active site with **2**. Protein is represented in green with residues forming van der Waals interactions and polar contacts (black dashed lines). Also three histidine residues coordinating the zinc ion are shown. Strands of the central β -sheet are labeled S4–S8. Compound **2** is shown in sticks with the $2F_o - F_c$ electron density map contoured at 0.8σ .

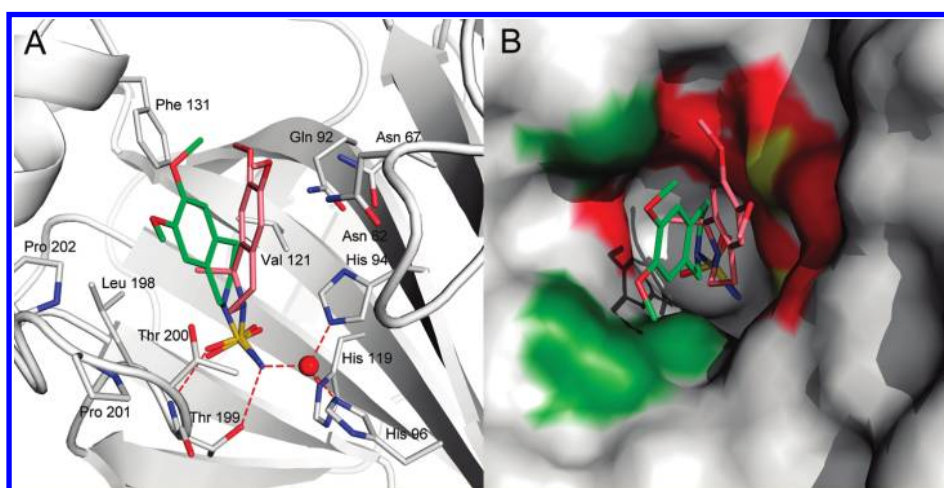


Figure 2. Comparison of **1** and **2** binding mode into the hCA II active site. Superposition of the complex structures is based on the best fit for C α atoms of hCA II residues 6–261. Compound **1** is represented with green carbon atoms, while **2** carbon atoms are salmon colored. In (A), the protein is represented by a ribbon and residues involved in the binding of the inhibitor compounds are shown as sticks. Polar interactions between the histidine residues coordinating the Zn ion (red sphere) and also the polar interactions between sulfonamide group and Thr 199 are indicated with dashed lines. (B) shows a top view into the active site where the protein is represented by its van der Waals radii. Atoms making contacts with the isoquinoline moiety of **1** and **2** are highlighted. Atoms within 4.0 Å from **1** and **2** are highlighted in green and red, respectively. Atoms colored yellow make contacts with both compounds. Atoms involved in contacts with the sulfonamide groups are not highlighted.

of the catalytic site and also with residues Ser197–Pro202 located in the loop connecting β -strands S3 and S4. Also, the side chain of Phe131 from helix 4 contributes to interaction with the substituting methoxy groups (Figure 2A, Table S1 in Supporting Information). In contrast, the substituted isoquinoline moiety of **2** is stabilized by the amino acid residues coming from the central part of the strands S6–S8 of the 10-stranded β -sheet¹ located on the opposite side of the active site cavity (residues Asn 62, Asn 67, Gln 92, Val 121; Figure 2A, Table S1 in Supporting Information). The methyl substituent on the isoquinoline scaffold

interacts with Leu 198 from the loop connecting β -strands S3 and S4.

Comparison of the residues interacting with **1** and **2**, respectively, revealed that the isoquinoline moiety can achieve two different binding modes within the hCA II active site and engage different amino acid residues in the interaction (Figure 2B). This finding is quite striking considering that **1** and **2** are very similar in their structure and also in their inhibitory properties (see Table 1).

We have compared the binding modes of **1** and **2** to other hCA II inhibitors that are structurally similar to our isoquinoline

Table 2. Crystal Parameters, Data Collection, and Refinement Statistics

parameter	complex of hCA II with 2
space group	P2 ₁
unit cell params	
<i>a</i> (Å)	42.18
<i>b</i> (Å)	41.21
<i>c</i> (Å)	72.00
α (deg)	90
β (deg)	104.31
γ (deg)	90
no. molecules in AU	1
wavelength (Å)	0.954
resolution range (Å)	26.62–1.47 (1.51–1.47)
no. unique refls	40 809
redundancy	3.6 (3.4)
completeness (%)	99.8 (99.8)
<i>R</i> _{merge} ^a	0.053 (0.238)
average <i>I</i> /σ(<i>I</i>)	7.8 (3.0)
Wilson <i>B</i> (Å ²)	13.7
refinement statistics	
resolution range (Å)	25.27–1.47 (1.51–1.47)
no. refls in working set	38 750 (2850)
no. refls in test set	2045 (132)
<i>R</i> ^b (%)	14.3 (18.6)
<i>R</i> _{free} ^c (%)	17.5 (22.4)
rmsd bond length (Å)	0.014
rmsd angle (deg)	1.69
no. atoms in AU	2511
no. protein–inhibitor atoms in AU	2171
no. solvent molecules in AU	340
mean <i>B</i> (Å ²)	13.8
PDB code	3PO6

^a $R_{\text{merge}} = \frac{\sum_{\text{hkl}} \sum_i |I_i(\text{hkl}) - \langle I(\text{hkl}) \rangle|}{\sum_{\text{hkl}} \sum_i I_i(\text{hkl})}$, where the $I_i(\text{hkl})$ is an individual intensity of the *i*th observation of reflection *hkl* and $\langle I(\text{hkl}) \rangle$ is the average intensity of reflection *hkl* with summation over all data. ^b $R = \frac{||F_o| - |F_c||}{|F_o|}$, where F_o and F_c are the observed and calculated structure factors, respectively. ^c R_{free} is equivalent to *R* value but is calculated for 5% of the reflections chosen at random and omitted from the refinement process.

sulfonamide series. For our analysis, we chose 59 crystal structures of hCA II in complex with inhibitors containing a cyclic or heterocyclic moiety attached directly to the sulfonamide group (Tables S2 and S3 in Supporting Information). Of these, 51 compounds displayed a binding mode highly similar to that of **1**. Eight compounds displayed a slightly altered binding mode in which the inhibitor position was shifted toward the β-strands S7 and S8. Nevertheless, none of the analyzed structures showed a binding mode overlapping with **2**. This analysis also revealed that a change in inhibitor binding in response to such a small structural change in the inhibitor is unique for our isoquinoline-sulfonamide compounds.

CONCLUSIONS

Comparison of the crystal structures of hCA II in complex with **1** and **2**, respectively, provided structural information about interactions of 1,2,3,4-tetrahydroisoquinolin-2-ylsulfonamides

with the hCA II active site. Although both compounds exhibit similar inhibitory potency toward hCA II, a unique binding mode of the **2** has been observed in response to the presence of a substituent on C-1 on the isoquinoline scaffold. The same inhibitory potency can apparently be achieved by two different binding modes of the inhibitor into the enzyme active site cavity. From a structural point of view, **1** and **2** served as excellent molecular tools for the detailed mapping of active site cavity. These results will be exploited for the rational design of molecules which could be highly selective inhibitors for various hCA isozymes.

EXPERIMENTAL SECTION

Detailed experimental procedures are given in the Supporting Information. Briefly, the crystals of human hCA II in complex with **2** (6,7-dimethoxy-1-methyl-1,2,3,4-tetrahydroisoquinolin-2-ylsulfonamide) were obtained by adding a 5-fold molar excess of the inhibitor (in dimethylsulfoxide) to a 10 mg/mL protein solution of hCA II (Sigma). The crystallization was performed in hanging drops at 18 °C in 0.1 M Tris-Cl, pH 8.2, 2.5 M (NH₄)₂SO₄, and 0.3 M NaCl. Diffraction data for hCA II in complex with **2** were collected at the Hamburg DESY, beamline X12. The structure of hCA II–**2** complex was solved using the difference Fourier method, using hCA II structure (Protein Data Bank entry 1H9N²¹) as the initial model. Atomic coordinates and experimental structure factors have been deposited with the Protein Data Bank with the code 3PO6. All figures showing structural representations were prepared with the programs PyMOL (DeLano Scientific; <http://www.pymol.org>). Crystal parameters and data collection statistics are summarized in Table 2. Compounds **1** and **2** were synthesized following previously reported procedures, and the spectral data were in accordance with the literature.¹³

ASSOCIATED CONTENT

S Supporting Information. Crystallization conditions, data collection, structure determination, refinement procedures, table of contacts between hCA II and **1** and **2**, respectively, and analysis results of the inhibitor binding mode in 59 hCA II structures. This material is available free of charge via the Internet at <http://pubs.acs.org>.

Accession Codes

[†]PDB codes for the hCA II structures are 3IGP and 3PO6.

AUTHOR INFORMATION

Corresponding Author

*Phone: +420220183210. Fax: +420220183144. E-mail: rezacova@img.cas.cz.

ACKNOWLEDGMENT

We thank the X12 beamline staff at the DESY synchrotron radiation facility for expert assistance during data collection. Financial support for this research was awarded by the Academy of Sciences of the Czech Republic (Projects AV0Z50520514 and AV0Z40550506), by Grant Agency of the Czech Republic (Grant GA203/09/0820), and by MiUR (Prin2008, Grant 20085HR5JK_002). This work was also financed in part by the FP7 EU project (Metoxia) to C.T.S. The authors thank Devon Maloy for critical proofreading of the manuscript.

■ REFERENCES

- (1) Krishnamurthy, V. M.; Kaufman, G. K.; Urbach, A. R.; Gitlin, I.; Gudiksen, K. L.; Weibel, D. B.; Whitesides, G. M. Carbonic anhydrase as a model for biophysical and physical-organic studies of proteins and protein–ligand binding. *Chem. Rev.* **2008**, *108*, 946–1051.
- (2) Mincione, F.; Scozzafava, A.; Supuran, C. T. The development of topically acting carbonic anhydrase inhibitors as anti-glaucoma agents. *Curr. Top. Med. Chem.* **2007**, *7*, 849–854.
- (3) Supuran, C. T. Carbonic anhydrases as drug targets—an overview. *Curr. Top. Med. Chem.* **2007**, *7*, 825–833.
- (4) Supuran, C. T. Carbonic anhydrases: novel therapeutic applications for inhibitors and activators. *Nat. Rev. Drug Discovery* **2008**, *7*, 168–181.
- (5) Supuran, C. T. Carbonic anhydrase inhibitors. *Bioorg. Med. Chem. Lett.* **2010**, *20*, 3467–3474.
- (6) Parkkila, S.; Parkkila, A. K.; Rajaniemi, H.; Shah, G. N.; Grubb, J. H.; Waheed, A.; Sly, W. S. Expression of membrane-associated carbonic anhydrase XIV on neurons and axons in mouse and human brain. *Proc. Natl. Acad. Sci. U.S.A.* **2001**, *98*, 1918–1923.
- (7) Thiry, A.; Dogne, J. M.; Supuran, C. T.; Masereel, B. Carbonic anhydrase inhibitors as anticonvulsant agents. *Curr. Top. Med. Chem.* **2007**, *7*, 855–864.
- (8) Asiedu, M.; Ossipov, M. H.; Kaila, K.; Price, T. J. Acetazolamide and midazolam act synergistically to inhibit neuropathic pain. *Pain* **2010**, *148*, 302–308.
- (9) Swietach, P.; Patiar, S.; Supuran, C. T.; Harris, A. L.; Vaughan-Jones, R. D. The role of carbonic anhydrase 9 in regulating extracellular and intracellular pH in three-dimensional tumor cell growths. *J. Biol. Chem.* **2009**, *284*, 20299–20310.
- (10) Winum, J. Y.; Rami, M.; Scozzafava, A.; Montero, J. L.; Supuran, C. Carbonic anhydrase IX: a new druggable target for the design of antitumor agents. *Med. Res. Rev.* **2008**, *28*, 445–463.
- (11) Thiry, A.; Supuran, C. T.; Masereel, B.; Dogne, J. M. Recent developments of carbonic anhydrase inhibitors as potential anticancer drugs. *J. Med. Chem.* **2008**, *51*, 3051–3056.
- (12) Tunuguntla, H. S.; Jorda, M. Diagnostic and prognostic molecular markers in renal cell carcinoma. *J. Urol.* **2008**, *179*, 2096–2102.
- (13) Gitto, R.; Agnello, S.; Ferro, S.; De Luca, L.; Vullo, D.; Brynda, J.; Mader, P.; Supuran, C. T.; Chimirri, A. Identification of 3,4-dihydroisoquinoline-2(1H)-sulfonamides as potent carbonic anhydrase inhibitors: synthesis, biological evaluation, and enzyme–ligand X-ray studies. *J. Med. Chem.* **2010**, *53*, 2401–2408.
- (14) Gitto, R.; Agnello, S.; Ferro, S.; Vullo, D.; Supuran, C. T.; Chimirri, A. Identification of potent and selective human carbonic anhydrase VII (hCA VII) inhibitors. *ChemMedChem* **2010**, *5*, 823–826.
- (15) Sippel, K. H.; Robbins, A. H.; Domsic, J.; Genis, C.; Agbandje-McKenna, M.; McKenna, R. High-resolution structure of human carbonic anhydrase II complexed with acetazolamide reveals insights into inhibitor drug design. *Acta Crystallogr., Sect. F: Struct. Biol. Cryst. Commun.* **2009**, *65*, 992–995.
- (16) D'Ambrosio, K.; Masereel, B.; Thiry, A.; Scozzafava, A.; Supuran, C. T.; De Simone, G. Carbonic anhydrase inhibitors: binding of indanesulfonamides to the human isoform II. *ChemMedChem* **2008**, *3*, 473–477.
- (17) Eriksson, A. E.; Jones, T. A.; Liljas, A. Refined structure of human carbonic anhydrase II at 2.0 Å resolution. *Proteins* **1988**, *4*, 274–282.
- (18) Supuran, C. T.; Scozzafava, A.; Casini, A. Carbonic anhydrase inhibitors. *Med. Res. Rev.* **2003**, *23*, 146–189.
- (19) Winum, J. Y.; Scozzafava, A.; Montero, J. L.; Supuran, C. T. Sulfamates and their therapeutic potential. *Med. Res. Rev.* **2005**, *25*, 186–228.
- (20) Srivastava, D. K.; Jude, K. M.; Banerjee, A. L.; Haldar, M.; Manokaran, S.; Kooren, J.; Mallik, S.; Christianson, D. W. Structural analysis of charge discrimination in the binding of inhibitors to human carbonic anhydrases I and II. *J. Am. Chem. Soc.* **2007**, *129*, 5528–5537.
- (21) Lesburg, C. A.; Huang, C.; Christianson, D. W.; Fierke, C. A. Histidine → carboxamide ligand substitutions in the zinc binding site of carbonic anhydrase II alter metal coordination geometry but retain catalytic activity. *Biochemistry* **1997**, *36*, 15780–15791.